A Multi-Wavelength Brillouin Fiber Laser of a Widely Tunable Profile Gain Raman Pumping

B. A. Ahmad[1] , Mohammed H.Khaleel[2] , Majid H.Alsadi[3]
[1,2,3]Al-Ma'moon University College Communication Engineering Department
Baghdad-Iraq
[1]belalanwer@almamonuc.edu.iq
[2]mohammed.h.khaleel@almamonuc.edu.iq
[3]mhnard@yahoo.com

Abstract

This paper presents a realization of a high input pumping Raman Power (RP) multi-wavelength Brillouin Fiber Laser (BFL) with a single Brillouin spacing line at room temperature. A traditional ring cavity fiber of extremely nonlinear properties, as a Brillouin Gain Medium (BGM) of 2km length, and a 3-dB coupler are engaged for single line spacing (odd-ordered) and Brillouin frequency shift Stokes distinctions. A numerical simulation based on Finite Element Method of Multiphysics COMSOL software algorithms is conducted to discuss the obtained results theoretically. From the obtained results, it is indicated that at Brillouin Pumping (BP) power of 8 dBm and RP power of 900 mW, 130 single spacing comb lines are formed with a channel wavelength spacing of 0.0782 nm. Moreover, it is noticed by reducing the RP power and the BGM length, an observable reduction is taken place in the lines number.

Nevertheless, it is observed that the proposed BFL can be widely tuned in C and L-bands within a wavelength sweeping from 1550nm to 1620nm.

Index terms: BFL, multi-wavelength, nonlinear effects.

1. INTRODUCTION

Nonlinear effects in optical fibers were examined by different research societies extensively for wide ranges of applications including the multi-wavelength fiber lasers [1]. For example, a ring cavity based highly nonlinear fibers was used in [2] as a parametric amplifying medium at four different wavelengths. In [3], experimentally, an investigation was demonstrated to study the performance of L-band multi-wavelength Brillouin–Raman fiber laser to utilize the nonlinear effects. A multi-wavelength erbium-doped fiber laser based on a nonlinear amplifying loop mirror was examined experimentally in [4]. In [5], a simple Brillouin-Raman multi-channel fiber laser was proposed with Rayleigh scattering support in without employing a feedback mirror. An all-fiber passively mode-locked soliton fiber laser based a nonlinear polarization rotation was proposed in [6].

Later, different approaches were proposed for producing multi-wavelength lasing effects at room temperature [7]. Most of these methods were conducted based Erbium doped fiber amplifier [8], semiconductor amplifier [9], and/ or Raman amplifier [10]. The use if such amplification techniques were introduced inside the laser cavity to advance the nonlinear effects of the optical fibers such as stimulated Brillouin scattering (SBS) [11], Rayleigh scattering (RS) [12], and stimulated Raman scattering (SRS) [13] to achieve high comb lines [14]. In other word, the additional gain was provided by those amplification techniques in the cavity to compensate the cavity loses and to generate multiple Stokes lines [14]. For instance, multi-wavelength BFL takes the essential advantages of narrow line-width, fixed Stokes channel spacing, and wide tunable wavelengths [15]. Therefore, to increase the oscillating power in the cavity, multi-wavelength Brillouin erbium fiber laser was suggested in [15] to ensure a rapid reduction in the erbium gain depletion, Brillouin gain saturation, and Brillouin threshold of the single-mode fiber thereby leading to the generation of higher number Brillouin Stokes lines. The Multi-wavelength Brillouin-Erbium Fiber Laser (MBEFL) uses a combination of Brillouin and erbium gains together in an optical fiber in order to generate multi-wavelength lasers [16]. Nonetheless, the MBEFL is a limited tuning range because the Stokes lines generation is only efficient within the free-running cavity mode operation wavelength [7]. Recently, tremendous interest was also directed on Brillouin-Raman fiber lasers (BRFL) [17]. These laser structures use both Brillouin and Raman gains for generating multi-wavelength lasers [18]. Another research on multi-wavelength fiber laser was applied on expanding the tuning range and increasing the number of pure channels with focusing on line spacing between the generated Stokes signals [19].

In this work, a realization of a high input pumping Raman Power (RP) multi-wavelength Brillouin Fiber Laser (BFL) with a single Brillouin spacing line at room temperature is proposed. Therefore, the experimental setup is discussed in section 2. In section 3, the authors discuss the obtained results from both numerical and experimental measurements. The paper is concluded in section 4.

2. EXPERIMENTAL SETUP AND MEASUREMENTS

Figure 1 illustrates the setup of the proposed BFL which is based on RP with dual multi-wavelength outputs of different channel spacing. A tuning laser source (TLS) of 200 kHz line width is introduced to act as an external BP power. Then, a 12 m long Erbium doped fiber (EDF) is conducted to the TLS and pumped with maximum 2 W at 1455 nm RP through a Wavelength Division Multiplexing (WDM) to realize the Brillouin pump signal amplification. The 3-ports circulator is conducted to launch the BP signal into a BGM in the fiber ring cavity and to perform unidirectional BP power lunching. The generated BS signal is monitored directly to the Optical Spectrum Analyzer (OSA). The circulator provides 54 dB isolation with an insertion loss of 0.5 dB during the operation wavelength range from 1520 nm to1620 nm. The fiber ring cavity is constructed from a 3-dB coupler and two different HNLF pieces length of 2 km and 500 m as BGM for multi-wavelength production. The HNLF pieces properties are listed in Table I for both 2 km and 500 m length.

Properties	2 km length	500 m length
Nonlinear coefficient	$10.8(w.km)^{-1}$	$11.5\ (w.km)^{-1}$
Attenuation factor	0.75 dB/km	0.82 dB/km
Effective area	12.4 μm²	11.6 μm²
Cut off wavelength	1250 nm	1180 nm
Dispersion constant	0.5 ps/(nm.km)	-0.1 ps/(nm.km)

Table 1. The HNLF properties.

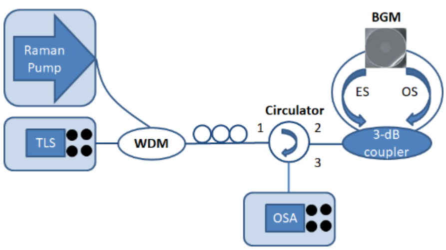

Figure 1. The proposed configuration for MWBFL setup.

From the proposed setup, the promised achievements can be described as follows: The 1st Brillouin Stokes line (BS1) can be generated when the amplified Brillouin input power goes beyond the Brillouin threshold condition inside the BGM. Next, the BS1 is circulated in a clockwise (CW) towards the 3-dB coupler to operate at new wavelength when is shifted by 0.08 nm from the BP wavelength with the opposite direction of the input BP signal. Therefore, the BS1 is divided into two parts symmetrically when propagating through the 3-dB bi-directional coupler; one part is coupled to OSA. The second part of the Stokes line propagates inside the ring cavity for the BFL generation by feeding it back into the BGM in CW direction with 0.08 nm frequency downshift from the BP wavelength to initiate BS2 after the BS1 power exceeds the Brillouin threshold condition of the BGM. The BS2 is subjected to another Brillouin frequency downshifter of 0.08 nm and oscillates in counter clockwise (CCW) direction in the ring cavity mode to generate SB3 in the opposite direction. The process repeats continuously to eliminate the high order modes below the threshold condition for the SBS effects.

In the ring cavity, four-wave-mixing (FWM) is amplified by Raman gain. Therefore, when the EDF gain reaches the saturation, the residual RP power will be inserted inside the BGM through the 3-dB coupler. During the circulation inside the BFL cavity and due to the bi-directional circulations for BP and the backscattering lines inside the BGM, FWM process is excited and amplified. Hence, all the circulated SBS Stokes lines in the CW direction and the reflected power signals from terminal fiber are monitored on OSA. Thus, the output Stokes lines at OSA are single spacing. RS is normally generated with same frequency of the pump wave at the opposite direction, but it is buried by SBS in the fiber because the gain coefficient of SBS for both direction inside the ring cavity is higher than RS [20]. Due to the bi-directional circulations for BP and the backscattering lines inside the BGM, FWM process is excited and contributed to generate the higher-order of Stokes and anti-Stokes channels consecutively.

3. RESULTS AND DISCUSSION

In Figure 2(a), the output power of BS1 signal with respect to the input BP power for the two different used BGM lengths is illustrated. During the experiment, the BP wavelength is fixed to 1560.9 nm and the output power is 8 dBm; while, the RP power is changed from 10 mW to 1000 mW, with a step of 100 mW. It is noticed that the threshold level for SB1 line decreases as the fiber length increases. For example, the BFL thresholds are found 40 mW and 10 mW for 500 m and 2 km of the HNLF, respectively, as seen in Figure 2(a). Nevertheless, it is found in case of exceeding the injected power over the Brillouin threshold value, the BS1 power follows an exponential increase. Moreover, the maximum archived BS1 peak is found about 14.5 dBm for 500 m length and 14 dBm for 2 km length. Such difference in the obtained output power between the two used lengths is attributed to the difference in the characteristics between these two lengths with less cavity losses for the shorter BGM. The wavelength Brillouin shift of the first amplified RS signal with various input RP power is presented in Figure 2(b). It is found a wavelength shift fluctuation at low injected RP power; however, the single spacing in the wavelength shifts is more stable as the RP power increases over the threshold level. In this part of the research, a numerical simulation based on Matlab formulation using Finite Element Method (FEM) of Multiphysics COMSOL software technology is invoked to obtain the numerical results. As seen in Figure 2, a good agreement is obtained between the simulated and the measured results.

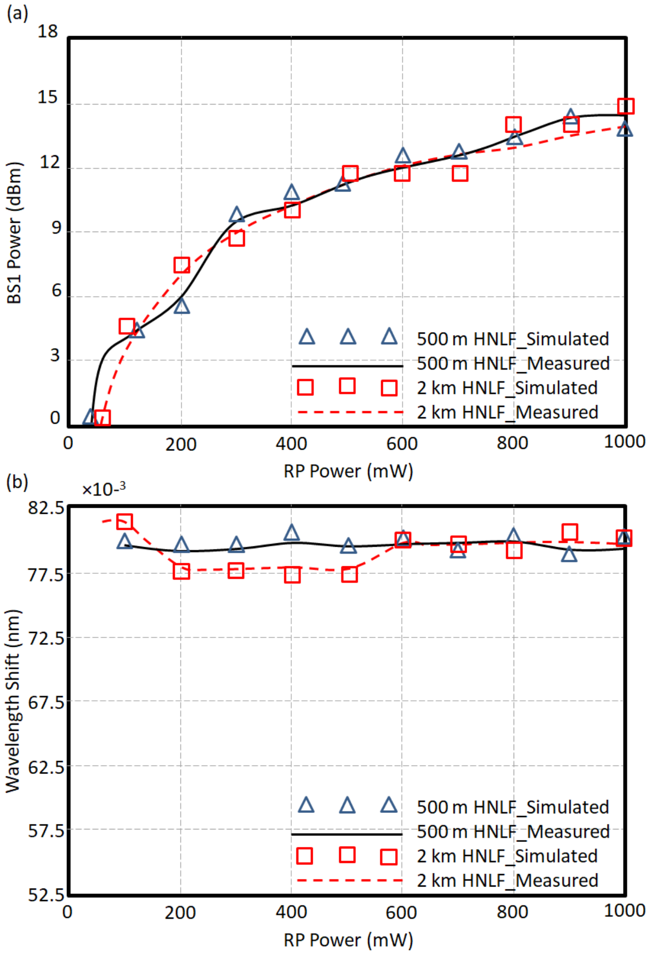

Figure 2. BS1 generated characteristics from the used HNLFs; (a) BS1 power change and (b) Wavelength shift.

This observation is attributed to the wavelength Brillouin frequency shift (v_B) which can be calculated from:

$$v_B = \frac{2n_p v_A}{2\lambda_p} \qquad (1)$$

where v_A is the acoustic velocity through BGM, n_p is the effective mode index at pump wavelength (λ_p). It is found that the Brillouin frequency shift is significantly affected with the fiber material factors v_A and n_p. Thus, the output channels in Figures 2 are shifted slightly, about 0.078nm, in HNLF. Nevertheless, an observable difference in the frequency shifts between different fiber lengths is attributed to the difference in the effective refractive index which is very sensitive to the fiber strain [15]. The output optical spectra for the odd Stokes lines are presented in Figure 3 as measured from OSA. In this experiment, the wavelength, BP, and RP power are fixed at 1560.9 nm, 8 dBm, and 1000 mW, respectively. As it is clearly seen, Figure 3 display a comb spectrum with single Brillouin frequency spacing of 0.0782 nm. The number of channels is observed to be increased as the HNLF lengths increase. For instance, 130 single spacing (70 Stokes and 60 anti-Stokes lines) are achieved at the 2 km HNLF lengths while 46 single spacing (27 Stokes and 19 Anti-stokes lines) are obtained as illustrated in Figure 3(a) and (b), respectively. This is attributed to the longer HNLF which has higher nonlinearity to promote the FWM effect and enhance the multi-wavelength generation process. It was also observed that each subsequent Stokes channel always has smaller power level than the previous one. This is due to the fact that the subsequent Stokes channels are initiated from the previous Stokes channels, the background levels of Figure 3 is observed to be relatively different.

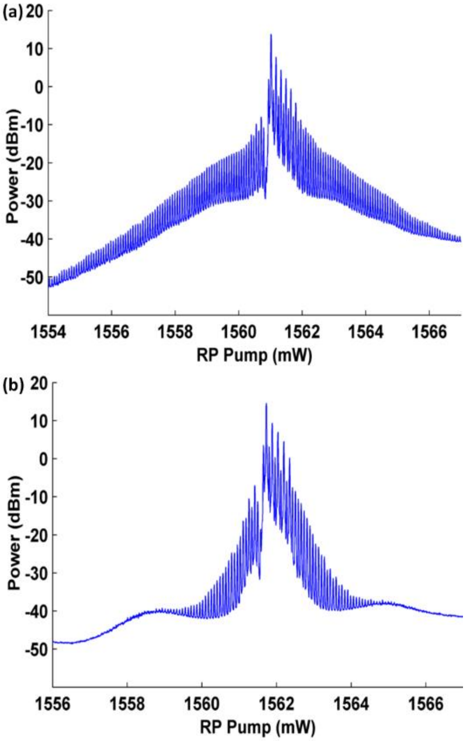

Figure 3. Output spectra of odd channels of the proposed MWBFL: (a) at 2 km and (b) at 500 m.

Figure 4 shows the number of output channels achieved by fixing the BP power at 8 dBm and varying the input RP power from 0 mW to 1000 mW on OSA. Experimentally, the comb lines with peak power above -30 dBm are considered only, while, all lines below this condition are considered noise. It is found from Figure 4, the order number of the Stokes lines increases as the RP increases; where, at RP power = 1W, 130

Stokes lines is obtained when the HNLF length is 2 km. However, the lines number is reduced to 40 lines when the HNLF length is 500m. This is attributed to Raman gain which is significantly is reduced by the gain medium length reduction. A Matlab code is based on Multiphysics COMSOL software algorithms is conducted to realize the number of stokes with RP power change according to the same measurement setup. It is found that the obtained numerical results agree very well with those measured results as presented in Figure 4.

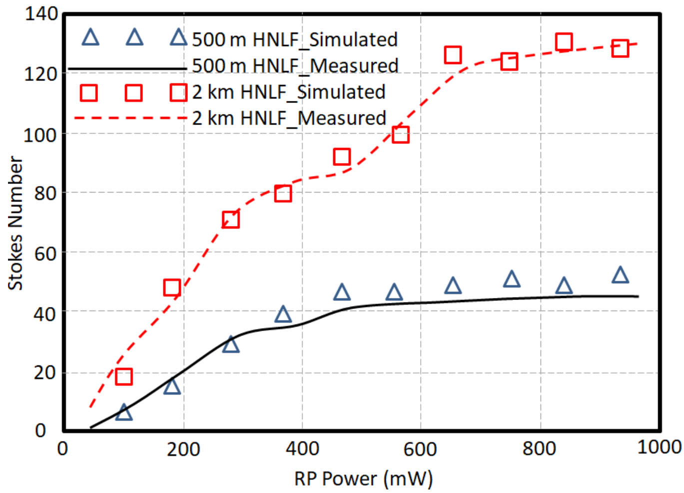

Figure 4. Number of output channels against RP powers for order BS.

Now, the profile gain range of RP based MWBFL is examined by tuning the BP wavelength from 1550 nm to 1620 nm with a step of 10 nm. Experimentally, at 1455 nm RP and BP powers are fixed to 1000 mW and 8 dBm, respectively. It is observed that the multi-wavelength fiber laser can be tuned within 70 nm wavelength without the presence of free-running EDF laser in the cavity. Figure 5 indicates a fixed BS provided by Raman pump and shows the number of Stokes of a MWBFL against BP wavelength for two different BGM lengths. At the HNLF length of 2 km, more than 110 odd-Stokes lines are obtained within a wavelength range from 1560 nm to 1610 nm. It is also observed that the Stokes lines disappear as the BP wavelength is tuned away from 1550 nm or 1620 nm wavelength. This is attributed to the Brillouin gain which is very low at this wavelength region and cannot support cascading process, accordingly.

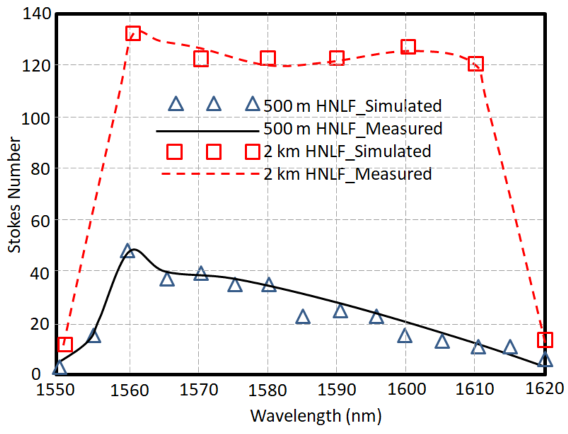

Figure 5. Gain spectrum.

4. Conclusions

A compact RP based MWBFL with widely tunable output of Brillouin frequency shift is experimentally and theoretically demonstrated in this article. The cascading of SBS and SRS play important roles with a simple ring cavity to generate the Stokes signal. It is concluded that the lower Stokes signal order modes are achieved by SBS. However, the high order channels are obtained from the multiple FWM process through the cavity mode. In comparison with various length of HNLF-based BFL, the 2km length is found to produce higher output lines number that the one based 500 m length. At BP power of 8 dBm and RP power of 900 mW, 130 lines of single spacing comb are generated along with a wide profile gain with a channel wavelength spacing of 0.0782 nm at the BGM length of 2km. The lines number is reduced by the RP power and the BGM length reduction. These findings are tested numerically to validate the archived results to find excellent agreements with measured results.

References

[1] Agrawal, G.P., Applications of nonlinear fiber optics. 2nd ed. Vol. 10. 2008: Academic press.

[2] Zamzuri, A., et al., All optical wavelength conversion based on degenerate four• wave mixing in Raman ring laser. Laser Physics Letters, 2011. 8(1): p. 62-65.

[3] Abass, A., et al., Characteristics of multi-wavelength L-band Brillouin–Raman fiber laser under forward and backward pumped environment. Journal of Applied Optics, 2013. 52(16).

[4] Liu, X., et al., Multiwavelength erbium-doped fiber laser based on a nonlinear amplifying loop mirror assisted by un-pumped EDF. Opt. Express, 2012. 20(7): p. 7088-7094.

[5] Sonee Shargh, R., et al., OSNR enhancement utilizing large effective area fiber in a multi-wavelength Brillouin Raman fiber laser. Laser Physics Letters, 2011. 8(2): p. 139-143.

[6] Shahabuddin, N.S., et al., Passively mode-locked soliton fiber laser using a combination of saturable absorber and nonlinear polarization rotation technique. Microwave and Optical Technology Letters, 2012. 54(6): p. 1430-1432.

[7] Abass, A., et al., An Overview of Multiwavelength Brillouin-Raman Fiber Laser. Journal of Advanced Laser and Optics Research, 2012. 1(1).

[8] Ceballos-Herrera, D., et al., Single-to three-wavelength switchable ytterbium-doped fiber laser based on intracavity induced loss by a long-period holey fiber grating. Optics &

Laser Technology, 2011. 43(4): p. 825-829.

[9] Dionísio, R.P., et al., 2 × 10 Gbit/s nonreturn-to-zero-ook to 10 Gbaud quasicontinuous phase modulation all-optical conversion using cascaded mach–zehnder interferometer-semiconductor optical amplifiers. Microwave and Optical Technology Letters, 2012. 54(5): p. 1240-1242.

[10] Pontes, M.J., et al., Brillouin effect characterization in all-Raman amplified 4 × 40 Gb/s WDM system. Microwave and Optical Technology Letters, 2012. 54(6): p. 1403-1407.

[11] Preda, C.E., A.A. Fotiadi, and P. Mégret, Numerical approximation for Brillouin fiber ring resonator. Opt. Express, 2012. 20(5): p. 5783-5788.

[12] Zamzuri, A.K., et al., Contribution of Rayleigh scattering on Brillouin comb line generation in Raman fiber laser. Applied optics, 2010. 49(18): p. 3506-3510.

[13] Frostig, H., et al., Single-pulse stimulated Raman scattering spectroscopy. Opt. Lett., 2011. 36(7): p. 1248-1250.

[14] Jinmei, L., et al., Optical Generation of Tunable Microwave Signal Using Cascaded Brillouin Fiber Lasers. Photonics Technology Letters, IEEE, 2012. 24(1): p. 22-24.

[15] Al-Mansoori, M.H., M. Ajiya, and M.A. Mahdi, L-Band Multiwavelength BEFL With Amplified Fiber Loop Mirror. Photonics Journal, IEEE, 2012. 4(2): p. 483-490.

[16] Martins, H., M. Marques, and O. Frazão, Comparison of Brillouin-Raman comb fiber laser in two different configurations. Laser physics, 2011. 21(11): p. 1925-1931.

[17] A. w. AI-Alimi, et al., Realization of Widely Tunable Brillouin

Erbium Doped Fiber Laser by using Brillouin Stokes Lines Feedback Control

[18] B.A.Ahmad, et al., Stable Double Spacing Multi-wavelength Brillouin-Erbium Doped Fiber Laser based on Highly Nonlinear Fiber. Laser physics, 2012. 22(5): p. 1-5.

[19] Zhu, T., X. Bao, and L. Chen, A self-gain random distributed feedback fiber laser based on stimulated Rayleigh scattering. Optics communications, 2012. 285(6): p. 1371-1374.

[20] A. M. R. Pinto, O. Frazão, Member, J. L.Santos, and M. Lopez-Amo, Multiwavelength Raman Fiber Lasers Using Hi-Bi Photonic Crystal Fiber Loop Mirrors Combined With Random Cavities. JOURNAL OF LIGHTWAVE TECHNOLOGY, 2011, 29(10): p. 1482-1488.